RESULTS OF VERTICAL TESTS FOR KEK-ERL 9-CELL SUPERCONDUCTING CAVITY

K. Umemori#, T. Furuya, H. Sakai, T. Takahashi, KEK, Tsukuba, Ibaraki, Japan
K. Shinoe, ISSP, University of Tokyo, Kashiwa, Chiba, Japan
M. Sawamura, JAEA, Tokai, Naka, Ibaraki, Japan

Abstract

In order to verify the technology needed for ERL main linac cavity, whose design is optimized for high current ERL operation, we fabricated a prototype of L-band 9-cell KEK-ERL superconducting cavity. After a series of surface treatment, such as annealing, electro-polishing, high-pressure-rinsing and baking, several vertical tests have been performed. As for cavity diagnostics, a rotating X-ray and temperature mapping system was constructed. The cavity performance was limited due to field emissions. The X-ray distributions were clearly observed by X-ray mapping system. In this report, we summarize the recent results of the vertical tests.

INTRODUCTION

At the ERL, stable operations are required for the superconducting cavities, with CW high current beam. This leads to stringent requirement against HOMs. Required features are following:

- Frequency 1.3 GHz
- Accelerating gradient 15~20 MV/m
- CW high current beam operation (> 100 mA)
- Energy recovery should work

There are two requirements against HOMs. One is suppression for the dipole and quadrupole HOMs. They can induce BBU instabilities, which cause the current limit and/or emittance growth. Another is requirement for monopole HOMs. They lead to heat loss at the HOM absorbers, which are located inside a cryomodule, at temperature of 80 K. Frequencies of monopole HOMs should be selected not to be close to the integral multiples of beam frequency.

KEK-ERL MODEL-2 CAVITY

As mentioned above, sufficient HOM suppression is required for the ERL main linac. To meet such conditions, we optimized cavity cell shapes and designed KEK-ERL model-2 cavity [1, 2]. Points of design are following.

(1) Cell shapes were optimized to HOM suppression. Diameter of iris was chosen to be 80 mm.
(2) Diameters of beampipes were selected to be 100 and 120 mm. All monopole and dipole HOMs can propagate to beampipes and are damped by RF absorbers.
(3) EFB (Eccentric-fluted beampipe) was applied, in order to damp quadrupole HOMs [3].

As a result, impedances of HOMs can be enough small. Current threshold against BBU instability is estimated to be several 100 mA [4].

#kensei.umemori@kek.jp

Table 1: Parameters for KEK-ERL Model-2 Cavity

Frequency	1.3GHz	Coupling	3.8 %
R_{sh}/Q	897 Ω	Geom.Fac.	289 Ω
E_{peak}/E_{acc}	3.0	H_{peak}/E_{acc}	42.5Oe/(MV/m)

Main parameters are listed in Table 1. Cell-to-cell coupling becomes large. This is a merit to keep field profile. The value R_{sh}/Q becomes around 900 Ω. A demerit is increase of E_{peak}/E_{acc}, which is 3.0. Enough suppression of field emissions is experimental issue.

In order to verify this cavity design, a proto-type of 9-cell KEK-ERL model-2 cavity was manufactured. It is shown in Figure 1. No stiffening rings were mounted at iris parts. Both flanges at the cavity ends were niobium. Vacuum seal was done using indium seal. Electron-beam-welded equator and iris parts were buffed with #400, in order to remove welding defects.

Figure 1: Proto-type of KEK-ERL model-2 cavity.

EXPERIMENTAL SETUP

Total of eight vertical tests have been performed at KEK-STF vertical test area. An input coupler was mounted on the upper flange of the cavity. Its coupling is variable. It can obtain matching condition while cooling down from 4K to 2K and also for all TM010 pass-band measurements. The history of surface treatments and vertical tests are shown in Table 2.

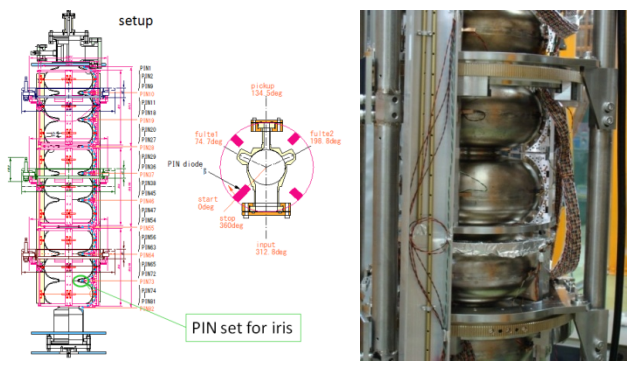

Figure 2: (Left) Layout of Si PIN diodes. (Right) Mapping system mounted on the cavity.

For the cavity diagnostics, many carbon resisters and Si PIN diodes are used to monitor temperature and X-rays. The left of Figure 2 shows the layout of the rotating mapping system and the right shows a part of it [5]. Array

of Si PIN diodes rotates by 360 degrees around the cavity surface and observes X-ray traces. Total of 82 Si PIN diodes are mounted for monitoring nine cells. Fixed mapping system was used from the 1st to the 3rd vertical tests, and the rotating mapping system was used from the 4th test.

Table 2: History of Vertical Tests and Surface Treatments

	Surface treatment	Maximum gradient at final state	Comment
Before vertical tests	EP(130 μm), Annealing, EP2(20 μm), HPR, Baking	---	---
1st test	---	15 MV/m	Field emission Many heat spot
2nd test	Baking	15 MV/m	Field emission Many heat spot
3rd test	HPR, Baking	15 MV/m	Field emission Many heat spot
4th test	EP2(50 μm), HPR, Baking	17 MV/m	Field emission A few heat spot
5th test	Nothing	16 MV/m	Field emission A few heat spot (same with 4th)
6th test	Local grinding EP2(50 μm), HPR, Baking	No data	Vacuum leak at connector
7th test	EP2(30 μm), HPR, Baking	10 MV/m	Dropped during pass-band measurement
8th test	EP2(20 μm), HPR, Baking	No data	Vacuum leak at connector

RESULTS OF VERTICAL TESTS

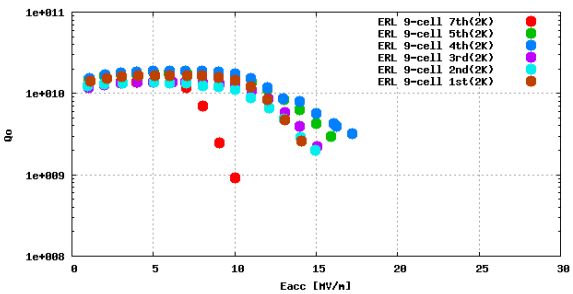

Figure 3 : Qo-Eacc curves of vertical tests.

The results of vertical tests are summarized in Figure 3. In this figure, plotted Qo and Eacc values are for final state, i.e. after processing / degrading. Typical residual resistance, estimated from Rs-1/T curve, was 15~20 nΩ.

Results from 1st to 3rd Vertical Tests

The 1st test was aimed to check the vertical test system. Before the 2nd test, only baking was done. Additional HPR was applied after the 2nd test. For these tests, field emission started below Eacc of 10 MV/m and fields were limited at 15 MV/m. The reason of field limitation was heating due to field emissions.

It is noted that behaviours of emission and temperature rise were much different between the 2nd and the 3rd vertical tests, while it was difficult to understand details from fixed type mapping system used for these three vertical tests.

Results from 4th and 5th Vertical Tests

Before the 4th test, additional EP was applied and removed 50 μm of surface. Hot bath rinsing, HPR, assembly and baking were done. The rotating mapping system was applied from the 4th test. After the 4th test, no surface treatment was done, since aim of the 5th test was to obtain detailed X-ray mapping data.

Again, field emission started below Eacc of 10 MV/m and fields were limited at 15~17 MV/m. The reason of field limitation was heating due to field emissions.

Figure 4 shows an example of X-ray mapping. This data was taken at Eacc of 13.9 MV/m at the 4th test. In the figure, "1-cell" is the cell which is close to the input port and "9-cell" is opposite side. The X-ray signal is strong around iris parts. There are two characteristic signals. One is a very strong and sharp peak, observed at 330 degree at iris between 8-cell and 9-cell. Looking at the details, clear X-ray trace can be seen. Another is a broad signals, observed around 150 degree, opposite side of sharp peak, at irises from 1-cell to 6-cell. These signals appeared at the same time around Eacc of 10 MV/m. The larger accelerating gradient, makes these signals stronger.

The X-ray mapping data was observed also for TM010 pass-band modes. Same sharp signal, at 330 degree of iris between 8-cell and 9-cell, could be seen for 8π/9, 7π/9, 6π/9-modes. The broad signals at irises around 1-cell to 6-cells were not seen this time. Probably, this was caused from the difference of the field patterns. For some other modes, X-ray signals appeared at different positions. Observed X-ray pattern changed according to the measured modes.

After the 5th measurement, inner surface of the cavity was observed using an inspection camera, so called Kyoto camera system [6]. A big tip was found, as shown in Figure 4, at 150 degree at the iris between 8-cell and 9-cell. Its size is several hundred μm diameter and several ten μm height. Though the surface inspection was also done after the 3rd vertical test, no such tip was observed. No such tips or dips were found at any other areas.

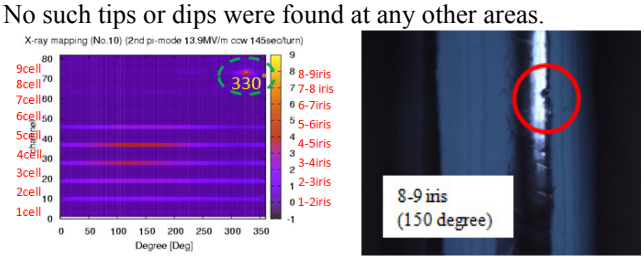

Figure 4: (Left) X-ray mapping data at Eacc=13.9 MV/m (Right) Inspection of cavity inner surface. A tip was found at iris between 8-cell and 9-cell.

It is very interesting that the tip was observed at just opposite side of the sharp X-ray peak observed on mapping. Most probably, this tip was the source of the

field emission for the 4th and the 5th vertical tests. This tip was removed by using local grinding system.

Results from 6th and 8th Vertical Tests

Unfortunately, vacuum leaks happened during measurements of the 6th and the 8th vertical tests. Situations are same for both cases. Strong radiations triggered the vacuum leaks at ceramics of N-connectors, which were located on the center of bottom flange. Leak rates were several 10^{-8} Pa m^3/s by hood method. Probably, they are small pin-holes.

At the 6th test, we measured π-mode, whose field was limited to 10 MV/m due to field emission. After that, we moved to 8π/9-mode measurement. There were some indications of processing. However, vacuum became bad. In the case of the 8th test, we measured π-mode at 4K. Strong emission was observed even at 7 MV/m. When trying to go further, vacuum leakage happened.

Results from 7th Vertical Test

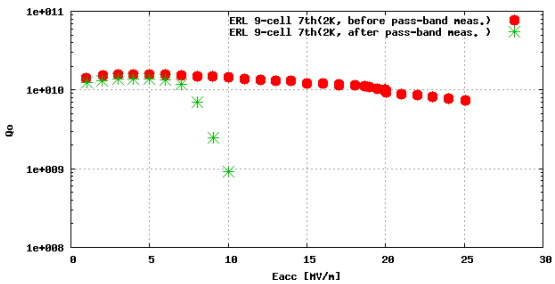

Figure 5: Qo-Eacc curves of 7th vertical tests. Red and green points are data before and after pass-band measurements, respectively.

After applying additional 30 μm EP, the 7th vertical test was performed. The results are shown in Figure 5. Red points are results measured just after cool down to 2K. It was very nice condition with small field emissions and Eacc reached to 25 MV/m. Field was limited by quench at the 2-cell equator, where temperature rise was observed and also two pits were found by inspection camera. After that, we did 6π/9-mode measurement. Eacc(at end cell) reached to more than 30 MV/m. Field was limited by quench at the 4-cell equator. After several quenches occurred and when another quench happened, it accompanied by abnormal X-ray burst. After that, field was limited to low and could not be recovered. Green points in Figure 5 are the data after pass-band measurements.

Figure 6 shows X-ray mapping data at irises for π-mode. Left plot is the data at 15 MV/m, Qo of 1.1e10, before degrading. No field emissions were observed. Right plot is the data at 7.7 MV/m, Qo of 6e9, after degrading. Strong X-ray signals were observed at many places of inside cavity.

More details can be seen in Figure 7. Left plot shows the X-rays observed at 6-cell, at 1π/9-mode, Eacc of 3 MV/m at end cell. Right plot is for X-rays observed at 8-cell, at 3π/9-mode, Eacc = 11 MV/m at end cell. Many traces can be clearly seen. At least more than ten field emission sources appeared after unfortunate X-ray burst.

After the vertical test, we inspected inside cavity, input coupler and flanges, but could not find any abnormal sign.

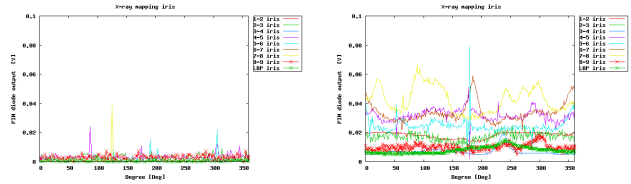

Figure 6: X-ray signals at irises. (Left) before and (Right) after pass-band measurements.

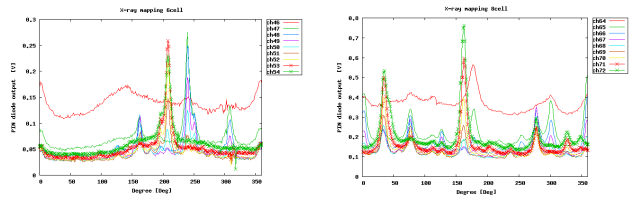

Figure 7: X-ray signals (Left) at 6-cell, observed at 1π/9-mode and (Right) at 8-cell, observed at 3π/9-mode.

SUMMARY

The HOM damped 1.3 GHz superconducting cavity was designed for the ERL main linac. Niobium 9-cell proto-type cavity was fabricated and vertical tests were performed after a series of surface treatments. At present, accelerating gradient is limited by field emissions. The rotating X-ray mapping system was constructed and worked well. Clear X-ray traces were observed.

REFERENCES

[1] K. Umemori et al., "Design of L-band superconducting cavity for the energy recovery linacs", APAC'07, Indore, India, Feb 2007, p. 570 (2007).

[2] K. Umemori et al., "Status of 9-cell superconducting cavity development for ERL project in Japan", SRF2009, Berlin, Germany, Sept 2009, p. 355 (2009).

[3] M. Sawamura et al., "Eccentric-fluted beam pipes to damp quadrupole higher-order modes", Phys. Rev. ST Accel. Beams 13 (2010) 022003.

[4] R. Hajima et al., "Analysis of HOM-BBU with newly designed cavities for a multi-GeV ERL light source", ERL'07, Daresbury, May 2007 (2007).

[5] H. Sakai et al., "Cavity diagnostics using rotating mapping system for 1.3GHz ERL 9-cell superconducting cavity", in these proceedings.

[6] Y. Iwashita et al., "Development of high resolution camera for observations of superconducting cavities", Phys. Rev. ST Accel. Beams 11 (2008) 093501.